

Revised result for the $^{32}\text{Cl}(p, \gamma)^{33}\text{Ar}$ reaction rate for astrophysical rp -process calculationsH. Schatz,^{1,2,3} C. A. Bertulani,^{1,*} B. A. Brown,^{1,2} R. R. C. Clement,^{1,2,†} A. A. Sakharuk,^{1,3} and B. M. Sherrill^{1,2,3}¹National Superconducting Cyclotron Laboratory, Michigan State University, East Lansing, Michigan 48824, USA²Department of Physics and Astronomy, Michigan State University, East Lansing, Michigan 48824, USA³Joint Institute for Nuclear Astrophysics, Michigan State University, East Lansing, Michigan 48824, USA

(Received 4 April 2005; revised manuscript received 20 October 2005; published 30 December 2005)

The $^{32}\text{Cl}(p, \gamma)^{33}\text{Ar}$ reaction rate is of potential importance in the rp process powering type I x-ray bursts. Recently, Clement *et al.* [Phys. Rev. Lett. **92**, 172502 (2004)] [1] presented new data on excitation energies for low-lying proton unbound states in ^{33}Ar obtained with a new method developed at the National Superconducting Cyclotron Laboratory. We use their data, together with a direct capture model and a shell model calculation, to derive a new reaction rate for use in astrophysical model calculations. In particular, we take into account capture on the first excited state in ^{32}Cl , and we also present a realistic estimate of the remaining uncertainties. We find that the $^{32}\text{Cl}(p, \gamma)^{33}\text{Ar}$ reaction rate is dominated entirely by capture on the first excited state in ^{32}Cl over the whole temperature range relevant in x-ray bursts. In the temperature range from 0.2 to 1 GK the rate is up to a factor of 70 larger than the previously recommended rate based on shell model calculations only. The uncertainty is now reduced from up to a factor of 1000 to a factor of 3 at 0.3–0.7 GK and a factor of 6 at 1.5 GK.

DOI: [10.1103/PhysRevC.72.065804](https://doi.org/10.1103/PhysRevC.72.065804)

PACS number(s): 26.50.+x, 21.60.Cs, 25.40.Lw, 27.30.+t

I. INTRODUCTION

Proton capture rates in the rapid proton capture process (rp process) play a critical role in determining energy release and final isotopic abundances in x-ray bursts [2–7]. Reliable rates are therefore important for quantitative interpretations of observations. For example, new highly accurate data on burst profile changes over periods of years as observed in GS 1826–24 [8] would provide unique constraints on x-ray burst models if the nuclear physics of the rp process would be well enough understood. As demonstrated in a number of x-ray burst model calculations [9–11] this is clearly not the case.

One problem is the reliability of proton capture rates in the rp process, especially in x-ray bursts where the reaction path runs close to the proton drip line. Far from stability, proton capture rates typically are governed by a few resonances and therefore statistical models are not applicable over the entire relevant temperature range of 0.2–2 GK [12]. However, shell model calculations in the sd [13,14] and fp shells [15–17] predict the properties of individual states but the typical uncertainty in level energies is about 100 keV, even for the calculations of level shifts from mirror states. This translates into uncertainties of three or more orders of magnitude in the reaction rates [1,18]. Currently, we expect that the majority of the proton capture rates in the rp process suffer from such uncertainties.

Clement *et al.* [1] recently developed a new experimental method using radioactive beams at the National Superconducting Cyclotron Laboratory at Michigan State University to accurately determine excitation energies of nuclei in the rp process path. They presented new results for the

excitation energies of states in ^{33}Ar that determine the $^{32}\text{Cl}(p, \gamma)^{33}\text{Ar}$ reaction rate. Based on the new experimental data we present here a reevaluation of the $^{32}\text{Cl}(p, \gamma)^{33}\text{Ar}$ rate, which is part of the reaction flow through the ^{30}S – ^{34}Ar region, an important bottleneck in the rp process in x-ray bursts that is possibly related to the observed double-peaked structure of some x-ray burst profiles [7].

The $^{32}\text{Cl}(p, \gamma)^{33}\text{Ar}$ reaction rate recommended in reaction rate compilations [19] and used in x-ray burst models so far was a ground-state capture rate based on shell model calculations with some experimental information from the ^{33}Ar mirror nucleus ^{33}P [14]. We use the new experimental data on states in ^{33}Ar together with shell model calculations and a direct capture model to derive a new dramatically improved rate for the $^{32}\text{Cl}(p, \gamma)^{33}\text{Ar}$ reaction. This differs from the initial discussion in Clement *et al.* [1] as we also take into account the contribution from proton capture on the first excited state in ^{32}Cl at 89.9 keV. This state is thermally populated in an astrophysical plasma and as we will show here actually dominates the proton capture rate on ^{32}Cl for the important temperature range between 0.2 and 1.5 GK. We also implement slight improvements in the penetrability calculations, evaluate the remaining shell model uncertainties, and present the reaction rate in a form usable by astrophysical reaction networks.

II. RESONANT CAPTURE

The resonant reaction rate for capture on a nucleus in an initial state i , $N_A \langle \sigma v \rangle_{\text{res } i}$, can for isolated narrow resonances be calculated as a sum over all relevant compound nucleus states j above the proton threshold [20]:

$$N_A \langle \sigma v \rangle_{\text{res } i} = 1.540 \times 10^{11} (\mu T_9)^{-3/2} \times \sum_j \omega \gamma_{ij} e^{-E_{ij}/(kT)} \text{ cm}^3 \text{ s}^{-1} \text{ mol}^{-1}, \quad (1)$$

*Current affiliation: Department of Physics, University of Arizona, Tucson, AZ 85721, USA.

†Current affiliation: Lawrence Livermore National Laboratory, 7000 East Ave., Livermore, CA 94550, USA.

where the resonance energy in the center-of-mass system, $E_{ij} = E_j - Q - E_i$, is calculated from the excitation energies of the initial E_i and compound nucleus E_j state, and k is the Boltzmann constant. We adopt an experimental ground-state mass difference Q (reaction Q value) of 3.343 ± 0.007 MeV [21]. T_9 is the temperature in gigakelvins and μ is the reduced mass of the entrance channel in atomic mass units. The resonance strengths $\omega\gamma_{ij}$ are in millions of electron volts and can be calculated for proton capture as

$$\omega\gamma_{ij} = \frac{2J_j + 1}{2(2J_i + 1)} \frac{\Gamma_{pij}\Gamma_{\gamma j}}{\Gamma_{\text{total } j}}, \quad (2)$$

where J_i is the target spin and J_j , Γ_{pij} , $\Gamma_{\gamma j}$, and $\Gamma_{\text{total } j}$ are spin, proton decay width, γ -decay width, and total width of the compound nucleus state j . The total width is given by $\Gamma_{\text{total } j} = \Gamma_{\gamma j} + \sum_i \Gamma_{pij}$. The proton decay widths depend exponentially on the resonance energy and can be calculated from the proton spectroscopic factor C^2S_{ij} and the single-particle proton width $\Gamma_{\text{sp } ij}$ as $\Gamma_{pij} = C^2S_{ij}\Gamma_{\text{sp } ij}$. Here we calculated spectroscopic factors with the USD shell model as in Herndl *et al.* [14]. The single-particle proton widths for most states were calculated from an exact evaluation of the proton scattering cross section from a Woods-Saxon potential well. This method is more precise than the penetrability model used by Herndl *et al.* [14] and Clement *et al.* [1] but agrees with previous work within 20%. The γ widths Γ_{γ} were taken from Herndl *et al.* [14]. This is justified as new experimental level energies are only available for the lower lying resonances where $\omega\gamma$ is largely independent of Γ_{γ} as $\Gamma_{\gamma} \gg \Gamma_p$, and because for those states the changes in the γ widths are less than 20%. The resulting properties of the resonance states in ^{33}Ar are listed in Table I.

III. DIRECT CAPTURE

The contribution to the $^{32}\text{Cl}(p,\gamma)^{33}\text{Ar}$ rate from direct capture into bound states has been calculated with a potential model [22] using a Woods-Saxon nuclear potential (central + spin orbit) and a Coulomb potential of a uniform charge distribution. The nuclear potential parameters were determined

by matching the bound-state energies. Spectroscopic factors were calculated with the USD shell model as in Herndl *et al.* [14].

The direct proton capture rate $N_A \langle \sigma v \rangle_{\text{dci}}$ on the target nucleus in state i is usually parametrized in terms of the astrophysical S factor $S(E_0)$ (in MeV b) at the Gamov window energy E_0 [23]:

$$N_A \langle \sigma v \rangle_{\text{dci}} = 7.83 \times 10^9 \left(\frac{Z}{\mu T_9^2} \right)^{1/3} \times S_i(E_0) e^{-4.29(Z^2\mu/T_9)^{1/3}} \text{ cm}^3 \text{ s}^{-1} \text{ mol}^{-1}, \quad (3)$$

with Z being the charge number of the target nucleus. $S_i(E_0)$ is the sum of the individual S factors of the transitions from the initial state i into all bound states in the final nucleus. Table II lists the individual S factors found for transitions into the five bound states of ^{33}Ar from both the ^{32}Cl ground state and the first excited state as well as the total S factor. For ground-state capture, our total S factor agrees within 30% with the one derived by Herndl *et al.* [14] using the same spectroscopic factors.

IV. NEW REACTION RATE

The relative population of the target nucleus states in thermodynamic equilibrium is simply given by the Saha equation. The total reaction rate is then the sum of the capture rate on all thermally excited states in the target nucleus weighted with their individual population factors:

$$N_A \langle \sigma v \rangle = \sum_i (N_A \langle \sigma v \rangle_{\text{res } i} + N_A \langle \sigma v \rangle_{\text{dci}}) \frac{(2J_i + 1)e^{-E_i/kT}}{\sum_n (2J_n + 1)e^{-E_n/kT}}. \quad (4)$$

To obtain the total resonant reaction rate on a thermally excited target one can combine Eqs. (1), (2), and (4) and find [24]:

$$N_A \langle \sigma v \rangle = \sum_j N_A \langle \sigma v \rangle_{0j} \frac{1}{G(T)} \left(1 + \sum_{i>0} \frac{\Gamma_{pij}}{\Gamma_{p0j}} \right), \quad (5)$$

TABLE I. Properties of resonant states. Listed are spin and parity J^π , excitation energy E_x , center-of-mass resonance energy E_r , proton single-particle widths Γ_{sp} for angular momenta l , spectroscopic factors C^2S , proton-decay width Γ_p , γ -decay width Γ_{γ} , and the resonance strength $\omega\gamma$. The upper part is for ground-state capture; the lower part is for capture on the first excited state in ^{32}Cl .

J^π	$E_x(\text{MeV})$	$E_r(\text{MeV})$	Γ_{sp}		C^2S		$\Gamma_p(\text{eV})$	$\Gamma_{\gamma}(\text{eV})$	$\omega\gamma(\text{eV})$
			$l=0$	$l=2$	$l=0$	$l=2$			
$5/2^+$	3.364	0.021 ± 0.009		8.00×10^{-42}		2.90×10^{-2}	2.32×10^{-43}	1.77×10^{-2}	2.32×10^{-43}
$7/2^+$	3.456	0.113 ± 0.009		1.90×10^{-13}		3.00×10^{-3}	5.70×10^{-16}	1.94×10^{-3}	7.60×10^{-16}
$5/2^+$	3.819	0.476 ± 0.008		2.01×10^{-2}		4.30×10^{-2}	9.03×10^{-4}	1.54×10^{-2}	6.88×10^{-4}
$1/2^+$	4.190	0.847 ± 0.100	6.30×10^2	1.01×10^1	6.70×10^{-2}	3.40×10^{-2}	4.26×10^1	1.54×10^{-1}	5.11×10^{-2}
$3/2^+$	4.730	1.387 ± 0.100	2.50×10^4	6.30×10^2	3.00×10^{-3}	3.90×10^{-2}	9.96×10^1	8.48×10^{-2}	4.33×10^{-3}
$7/2^+$	3.456	0.023 ± 0.009		1.30×10^{-39}		4.64×10^{-3}	6.03×10^{-42}	1.94×10^{-3}	4.83×10^{-42}
$5/2^+$	3.819	0.386 ± 0.008	1.35×10^{-1}	1.50×10^{-3}	2.40×10^{-2}	4.39×10^{-1}	3.90×10^{-3}	1.54×10^{-2}	1.78×10^{-3}
$1/2^+$	4.190	0.757 ± 0.100		3.50		2.27×10^{-3}	7.94×10^{-3}	1.54×10^{-1}	5.73×10^{-6}
$3/2^+$	4.730	1.297 ± 0.100	1.60×10^4	3.80×10^2	7.49×10^{-2}	3.77×10^{-3}	1.20×10^3	8.48×10^{-2}	3.13×10^{-2}

TABLE II. Spectroscopic factors C^2S and astrophysical S factors $S(E_0)$ for direct capture into bound states in ^{33}Ar . Listed are results for capture on the ^{32}Cl ground state as well as on the first excited state in ^{32}Cl (denoted with an asterisk). J^π are spin and parity of the ^{33}Ar final state, n is the node number, l_0 is the single-particle orbital momentum, and j_0 is the total single-particle angular momentum. The table only includes the significant contributions to the total S factor.

E_x (MeV)	J^π	$(nl_0)_{j_0}$	C^2S	$S(E_0)$ (MeV b)	C^2S^*	$S(E_0)^*$ (MeV b)
0	$1/2^+$	$2s_{1/2}$	0.08	6.56×10^{-3}	1.13	4.45×10^{-3}
		$1d_{3/2}$	0.67	4.47×10^{-3}		
1.359	$3/2^+$	$2s_{1/2}$	0.19	1.78×10^{-3}	0.006	6.61×10^{-4}
		$1d_{3/2}$			0.12	6.80×10^{-4}
1.798	$5/2^+$	$2s_{1/2}$	0.15	1.84×10^{-3}	0.002	3.21×10^{-4}
		$1d_{3/2}$			0.62	4.72×10^{-3}
		$1d_{5/2}$			0.021	1.65×10^{-4}
2.439	$3/2^+$	$2s_{1/2}$	0.031	4.32×10^{-3}	0.024	1.99×10^{-3}
		$1d_{3/2}$	0.17	1.09×10^{-3}	0.13	5.01×10^{-4}
3.154	$3/2^+$	$2s_{1/2}$	0.068	1.02×10^{-2}	0.17	4.35×10^{-4}
		$1d_{3/2}$	0.52	2.21×10^{-3}		
Total				3.25×10^{-2}		1.39×10^{-2}

where j sums over all resonances in the compound nucleus; i sums over the thermally populated states in the target nucleus as long as the resonance energy $E_{ij} > 0$ with $i = 0$ being the ground state. $N_A \langle \sigma v \rangle_{0j}$ is the reaction rate contribution from ground-state capture via the resonance j . $G(T)$ is the temperature-dependent partition function of the target nucleus:

$$G(T) = (2J_0 + 1)^{-1} \sum_i (2J_i + 1) \exp(-E_i/kT). \quad (6)$$

This is similar to Eq. (10) in Fowler, Caughlan, and Zimmerman [25]. Equation (5) shows that for a given resonance the relative contribution from capture on each excited target state depends only weakly on temperature and the actual population of the excited state through the partition function $G(T)$. The contribution of excited states is mostly determined by the ratio of the proton widths to the excited state and to the ground state. Of course the temperature determines through $\langle \sigma v \rangle_{0j}$ the relative importance of the various resonances.

In this work we consider only capture on the ground state and the first excited state in ^{32}Cl . The ^{32}Cl ground state is experimentally known to have spin and parity 1^+ . The spin for the experimentally known first excited state at 89.9 keV has not been determined unambiguously but we assign a spin of 2^+ based on the level structure of the ^{32}P mirror and our shell model calculations. Excited states in the target will only play a role when for the relevant temperatures the thermal excitation time scale is smaller than the proton capture time scale. We can estimate the thermal excitation time scale for a γ -induced transition from the ground state to the first excited 2^+ state in ^{32}Cl by using the formalism of Ward and Fowler [26]. We assume a level lifetime of 280 ps from the mirror level in ^{32}P , which is an upper limit as the mirror state is 12 keV lower in excitation energy. We find that even for the lowest relevant temperatures of 0.2 GK the excitation time scale is of the order of 30 ns. Assuming typical x-ray burst conditions with a density of 10^6 g/cm 3 and a proton mass fraction of 0.7 the time scale for thermal excitation is always less than 0.2% of the proton capture time scale for all temperatures between

0.2 and 2 GK. Therefore, the first excited 2^+ state in ^{32}Cl is always in thermal equilibrium with the ground state and Eq. (5) applies.

What is the role of higher lying excited states in ^{32}Cl ? The second excited state in ^{32}Cl is located at an energy of 466.1 keV. At such a high excitation energy the proton decay width Γ_p in Eq. (5) is already drastically reduced for the low-lying resonances that have a significant ground-state capture rate $\langle \sigma v \rangle_{0j}$. Therefore, the capture rate on the second excited state in ^{32}Cl is negligible as either Γ_{p2j} or $\langle \sigma v \rangle_{0j}$ in Eq. (5) are small for all resonances. Similar arguments apply to higher lying states.

The contributions from individual resonances and direct capture to the total $^{32}\text{Cl}(p, \gamma)^{33}\text{Ar}$ reaction rate are shown in Fig. 1. The temperature-dependent relative population of the ground and first excited state in ^{32}Cl has been taken into account. Direct capture on the ground or the excited state is negligible over the entire relevant temperature range of 0.2–2 GK.

As Fig. 1 shows, the capture-rate contributions from ground and excited target states vary greatly as Γ_p depends strongly on proton energy, spin, and nuclear structure. For $^{32}\text{Cl}(p, \gamma)^{33}\text{Ar}$ the most dramatic change occurs for the $5/2^+$ 3.819-MeV resonance. For this resonance the spin of the excited state (2^+) is one unit larger than for the ground state (1^+), allowing for s -wave protons to populate the $5/2^+$ resonance in addition to d -wave protons. As a result the proton width for capture on the excited state is a factor of 4.3 larger than for ground-state capture despite the slightly lower proton energy. As a consequence [see Eq. (5)] the resonant capture on the first excited state in ^{32}Cl via the 3.819-MeV $5/2^+$ state in ^{33}Ar becomes the dominant contribution to the stellar $^{32}\text{Cl}(p, \gamma)^{33}\text{Ar}$ reaction rate for all relevant temperatures between 0.15 and 2 GK (see Fig. 1). This is despite the fact that the population of the first excited state in ^{32}Cl , for example, at 0.3 GK is only 5%. As Eq. (5) demonstrates, the relative importance of contributions from capture on various states in the target is largely independent of their

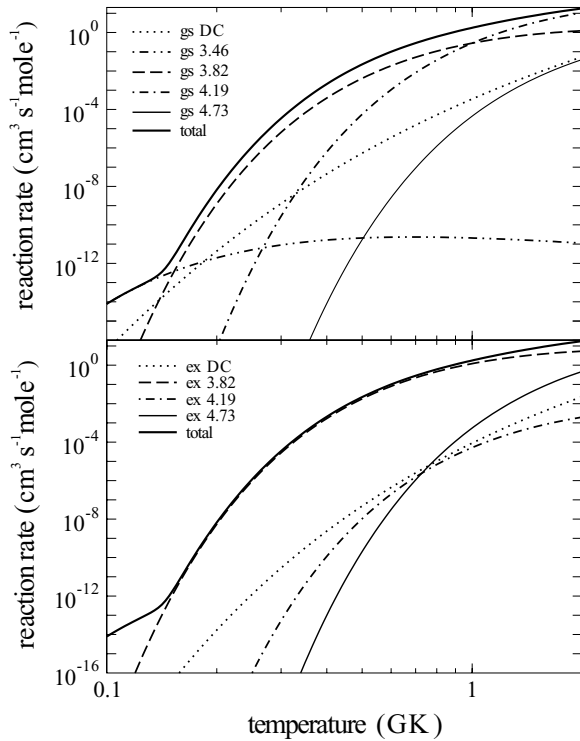


FIG. 1. The contributions of various individual resonances and through direct capture (DC) to the $^{32}\text{Cl}(p, \gamma)^{33}\text{Ar}$ reaction rate as functions of temperature. In the legend, resonances are labeled with their excitation energy in ^{33}Ar . The upper panel shows contributions from ground-state capture; the lower panel shows contributions from capture on the first excited state in ^{32}Cl in each case weighted with the relative population of the respective target state. In addition, both panels show the same total $^{32}\text{Cl}(p, \gamma)^{33}\text{Ar}$ reaction rate for comparison. Contributions from ground-state capture via the 3.36-MeV resonance and from capture on the first excited state via the 3.46-MeV resonance are too small to appear in this graph.

population (with the exception of their contribution to the partition function); what matters most is the proton width for the transition into the resonant state.

The remaining uncertainty from resonance energies ranges from 20 to 50% for the most important temperatures between 0.3 and 0.8 GK and increases to about a factor of 2 at 1.5 GK. It originates mainly from the small experimental uncertainties in the ^{33}Ar excitation energies and the reaction Q value. For the experimentally unknown higher lying levels we assume an uncertainty in the excitation energy of 100 keV, which is a typical deviation for shell model predictions of Coulomb shifts in this region. These levels only begin to contribute to the total reaction rate beyond around 1 GK and lead to the somewhat increased error at highest temperatures. At this level of error, other uncertainties in the shell model calculations now become relevant as well. The Woods-Saxon well used for the proton scattering widths is adjusted so that the total density for protons filled up to the Fermi energy reproduces the rms charge radius of nearby stable nuclei. We estimate an uncertainty of 5% in the Woods-Saxon radius parameter, which leads to a 15% uncertainty in the proton decay widths.

TABLE III. Spectroscopic factors C^2S for $d_{5/2}$ neutron removal from ^{34}Ar to various $5/2^+$ states in ^{33}Ar calculated with the shell; model effective interactions USD and USD05 and compared to experimental data [28] from the ^{34}S to ^{33}P mirror reaction for $d_{5/2}$ protons. The excitation energies E_x of the $5/2^+$ states are the experimentally known ones in the ^{33}P mirror.

E_x (MeV)	C^2S		
	Exp	USD05	USD
1.85	1.09	0.99	1.09
3.49	0.31	0.27	0.70
4.05	1.28	1.62	1.30
5.05	1.66	1.51	1.33

In principle one could estimate the uncertainty of the shell model spectroscopic factors by comparing calculated spectroscopic factors with experimental data. No experimental data are available for the relevant proton spectroscopic factors in ^{33}Ar or the corresponding neutron spectroscopic factors in the ^{33}P mirror. In addition, small spectroscopic factors are in general difficult to reliably extract from direct reaction cross sections owing to the possibility of multistep routes. However, we can test our shell model descriptions for the relevant states in ^{33}Ar by comparing their relatively large neutron spectroscopic factors for ^{34}Ar to ^{33}Ar neutron removal with experimental data for the mirror proton spectroscopic factors for ^{34}S to ^{33}P proton removal. We limit the discussion to the $5/2^+$ states, as the $^{32}\text{Ar}(p, \gamma)^{33}\text{Ar}$ reaction is dominated by the resonant contribution from the third $5/2^+$ state in ^{33}Ar . The calculations and experimental data for the $5/2^+$ states are summarized in Table III. The calculations are carried out with the original USD interaction as well as the close-to-final version of a new sd -shell interaction USD05 [27] obtained from a least-squares fit to about 600 levels in the sd -shell nuclei. The spectroscopic factors are all large numbers and in good agreement with the experimental data from the mirror reaction. When calculated levels can be matched to experimental levels with the present degree of accuracy (about 100 keV) the comparison in Table III shows that the largest calculated spectroscopic factors are accurate to about 20% and the moderately large spectroscopic factors (as for the second $5/2^+$ state) are accurate to about a factor of 2.

In addition, we can look at variations in spectroscopic factors calculated with different shell model effective interactions. The spectroscopic factors for the important $^{32}\text{Cl}(2^+)$ to $^{33}\text{P}(5/2^+)$ $l = 0$ transitions are shown in Table IV for the old USD interaction as well as the new USD05 interaction. All of the spectroscopic factors are small since the $s_{1/2}$ orbit is mostly filled in ^{32}Cl . The $l = 0$ spectroscopic factor summed over all final $5/2^+$ states is only 0.131 for USD05. The comparison of the two interactions in Table II shows that the largest of the spectroscopic factors (including the one to the third $5/2^+$ state of interest) agree to about 20%. Spectroscopic factors calculated with other effective interactions such as SDPOTA [29] or CWH [30], which also do a reasonable job of reproducing the energy levels for nuclei in the upper sd shell,

TABLE IV. $l = 0$ spectroscopic factors for the $5/2^+$ states in ^{33}Ar for proton capture on the 2^+ state in ^{32}Cl . Spectroscopic factors C^2S and excitation energies E_x calculated with the USD and the USD05 interaction are compared.

E_x (MeV)		C^2S	
USD05	USD	USD05	USD
1.99	2.00	0.0013	0.0006
3.42	3.83	0.0022	0.012
4.22	4.19	0.025	0.023
4.82	5.00	0.049	0.040
6.39	6.64	0.00002	0.0024
6.54	6.93	0.017	0.0024

show a similar behavior. In general, a small spectroscopic factor in the presence of other states with much larger spectroscopic factors may be very uncertain (as observed for many of the states in Table IV). However, when the spectroscopic factor is large compared to those for nearby states it can be relatively accurate. Thus the estimated theoretical error for small spectroscopic factors must be treated on a case-by-case basis.

In summary, the shell model can describe the neutron single-particle strength of the relevant states here within 20% to a factor of 2. In addition, the important $l = 0$ proton spectroscopic factor for the third $5/2^+$ state is relatively large compared to other states and the total $l = 0$ proton single-particle strength, and its calculation should therefore be relatively reliable. We therefore estimate a factor of 2 uncertainty in the shell model spectroscopic factor in this specific case. To take into account other uncertainties such as the previously discussed proton single-particle widths, we adopt a total uncertainty of a factor of 2.5 for the $^{32}\text{Cl}(p, \gamma)^{33}\text{Ar}$ reaction rate on top of the uncertainty from the resonance energies, which is accurately calculated as a function of temperature. The new reaction rate with its uncertainties is

TABLE V. Reaction rate $N_A(\sigma v)$ as a function of temperature T . Given is the recommended rate from this work (rec) as well as a lower and upper rates that reflect the estimated error bar.

T (GK)	$N_A(\sigma v)$ ($\text{cm}^3\text{s/mol}^{-1}$)		
	rec	lower	upper
0.1	7.85×10^{-15}	1.73×10^{-15}	2.81×10^{-14}
0.2	6.62×10^{-9}	3.20×10^{-9}	1.36×10^{-8}
0.3	3.44×10^{-5}	1.94×10^{-5}	6.04×10^{-5}
0.4	2.09×10^{-3}	1.27×10^{-3}	3.41×10^{-3}
0.5	2.21×10^{-2}	1.33×10^{-2}	3.67×10^{-2}
0.6	9.97×10^{-2}	5.80×10^{-2}	1.77×10^{-1}
0.7	2.82×10^{-1}	1.58×10^{-1}	5.37×10^{-1}
0.8	6.06×10^{-1}	3.27×10^{-1}	1.24
0.9	1.09	5.67×10^{-1}	2.39
1.0	1.76	8.75×10^{-1}	4.06
1.5	7.94	3.40	2.03×10
2.0	1.78×10	7.48	4.39×10

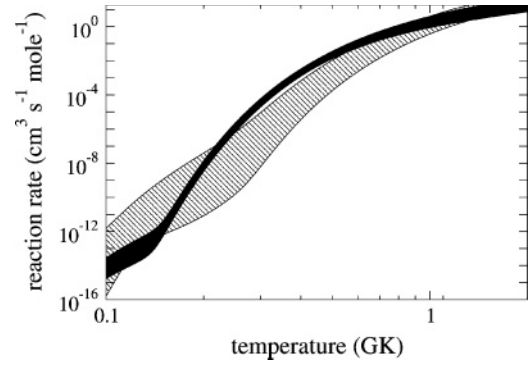


FIG. 2. Total $^{32}\text{Cl}(p, \gamma)^{33}\text{Ar}$ reaction rate from this work (solid area) and previous shell model rate without experimental data (hatched area). The width of the area reflects the estimated uncertainty.

tabulated in Table V and displayed in Fig. 2. The total estimated uncertainty of the rate ranges from about a factor of 3 at temperatures around 0.3–0.7 GK to about a factor of 6 at temperatures around 1.5 GK.

Often, reaction rates are implemented into reaction network codes using a fit of the form

$$N_A(\sigma v) = \sum_i \exp(a_{0i} + a_{1i}T_9^{-1} + a_{2i}T_9^{-1/3} + a_{3i}T_9^{1/3} + a_{4i}T_9 + a_{5i}T_9^{5/3} + a_{6i} \ln T_9), \quad (7)$$

which is, for example, used in the `reaclib` reaction rate library. In Table VI we give fit parameters a_{ni} for our new recommended $^{32}\text{Cl}(p, \gamma)^{33}\text{Ar}$ rate as well as for the upper and lower uncertainties. The fits are accurate to 5% and are valid between 0.1 and 10 GK. Beyond 2 GK we use the Hauser-Feshbach predictions from NON-SMOKER [31] using the procedure described by the NACRE Collaboration [32]. The low-temperature behavior is reasonable, so the fits can be used in model simulations that encounter lower temperatures.

V. DISCUSSION

Our ground-state capture rate for $^{32}\text{Cl}(p, \gamma)^{33}\text{Ar}$ is similar to the rate given by Clement *et al.* [1]. Small differences

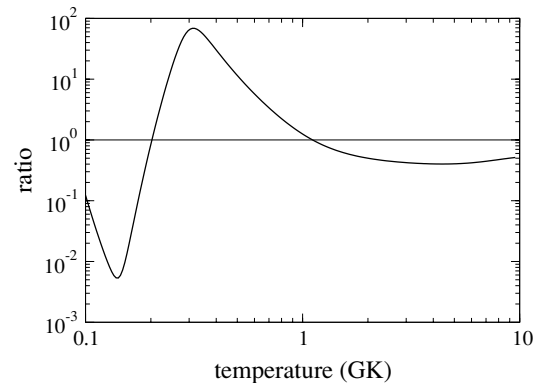


FIG. 3. Ratio of the $^{32}\text{Cl}(p, \gamma)^{33}\text{Ar}$ reaction rate of this work to the rate calculated by Herndl *et al.* [14].

TABLE VI. Fit coefficients [see Eq. (7)] for the recommended rate from this work (rec) as well as for the lower and upper limits that reflect the estimated error bar.

	a_0	a_1	a_2	a_3	a_4	a_4	a_7
Rec	0.150730×10 0.542869×10^2	-0.539842×10 -0.782163×10	-0.153745×10^2 0.367513×10^3	0.187918×10^2 -0.425108×10^3	0.126139×10 0.502875×10	-0.208373 0.823457	-0.134957×10^2 0.262097×10^3
Lower	0.551123×10^3 -0.517996×10^2	-0.158099×10^2 -0.156901×10	0.886227×10^3 -0.173733×10^3	-0.150891×10^4 0.237842×10^3	0.878013×10^2 -0.114259×10^2	-0.495734×10 0.538535	0.714263×10^3 -0.124462×10^3
Upper	0.299493×10^3 -0.269317×10^3	-0.143477×10^2 -0.794584	0.705984×10^3 -0.279531×10^3	-0.104556×10^4 0.597651×10^3	0.530983×10^2 -0.505961×10^2	-0.269508×10 0.399204×10	0.533394×10^3 -0.244496×10^3

arise from the slightly improved calculation of the proton single-particle widths, the comprehensive reevaluation of the shell model uncertainties, and the modifications in the proton widths by taking into account transitions into excited target states. The major change however comes from the consideration of the capture on the first excited state in ^{32}Cl . In the critical temperature range around 0.2–0.4 GK, where for typical x-ray burst conditions (densities of 10^5 – 10^6 g/cm 3 and hydrogen mass fractions of 0.1–0.7) the reaction rate becomes comparable to the burst time scales (10–100 s), our rate is a factor of more than 4 larger than the ground-state capture rate shown in Clement *et al.* [1]. In the same temperature range our rate is up to a factor of 70 larger than the recommended shell-model-based rate in Herndl *et al.* [14] (see Fig. 3).

The impact of thermally excited states in the target nucleus on a reaction rate is often expressed in terms of a “stellar enhancement factor” (SEF), which is defined as the ratio of the actual capture rate to the ground-state capture rate. Figure 4 shows the SEF determined in this work.

The enhanced proton capture rate from the first excited state in ^{32}Cl leads to a dramatic enhancement of the reaction rate of up to a factor of 5 at the important temperatures around 0.2–0.4 GK. Recent reaction rate compilations typically use SEFs that are calculated with the statistical Hauser-Feshbach model [19,32]. For comparison we also show in Fig. 4 the SEF obtained with the Hauser-Feshbach code NON-SMOKER [31].

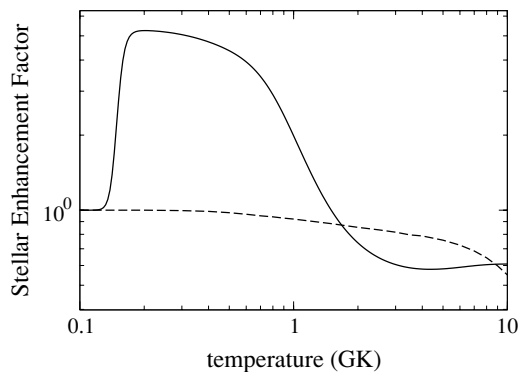


FIG. 4. Stellar enhancement factor derived in this work (solid line) and from the statistical model code NON-SMOKER (dashed line).

Clearly in this case a statistical approach to calculating the SEF does not give the correct result, even in the temperature range above 0.7 GK where strictly speaking the Hauser-Feshbach model is expected to be applicable [12,31]. This is no surprise as here the SEF is entirely dominated by the properties of a single resonance. However, this example illustrates that large uncertainties can be introduced when using statistical model SEFs far from stability when reaction rates are dominated by a few resonances only. A better general approach would be to calculate SEFs within the shell model.

Clearly accurate masses and excitation energies are the single most important step for improving the accuracy of theoretical reaction rates. For comparison Fig. 2 also shows the uncertainty band of the reaction rate for the case that none of the excitation energies would be known experimentally, a situation that is very common along the *rp*-process path. Clearly, without experimental excitation energies reaction rates in the *rp* process far from stability can be uncertain by many orders of magnitude. A measurement of excitation energies and Q values to better than 10 keV can reduce this uncertainty to about a factor of 3.

To obtain in critical cases even more precise reaction rates one would need to perform indirect measurements of spectroscopic factors, or perform a direct measurement of the reaction rate at astrophysical energies. Note, however, that in this particular case a direct measurement would not be possible as the reaction rate is dominated by capture on the first excited state in the ^{32}Cl target nucleus. This underlines the importance of indirect methods in determining accurate stellar reaction rates.

ACKNOWLEDGMENTS

We thank M. Wiescher for pointing out the importance of the time scale for thermal excitation and O. Sorlin for pointing out the potential relevance of the first excited state in ^{32}Cl . This work was supported by NSF Grant Nos. PHY-0110253 (NSCL) and PHY-0216783 (Joint Institute for Nuclear Astrophysics). H.S. acknowledges support through the Alfred P. Sloan Foundation. B.A.B. acknowledges support from NSF Grant No. PHY-0244453. C.A.B. acknowledges support by the U.S. Department of Energy under Grant No. DE-FG02-04ER41338.

- [1] R. R. C. Clement *et al.*, Phys. Rev. Lett. **92**, 172502 (2004).
- [2] R. K. Wallace and S. E. Woosley, Astrophys. J. Suppl. **45**, 389 (1981).
- [3] H. Schatz *et al.*, Phys. Rep. **294**, 167 (1998).
- [4] M. Wiescher, J. Görres, and H. Schatz, J. Phys. G Top. Rev. **25**, R133 (1999).
- [5] H. Schatz *et al.*, Nucl. Phys. **A654**, 924 (1999).
- [6] F.-K. Thielemann *et al.*, Prog. Part. Nucl. Phys. **46**, 5 (2001).
- [7] J. L. Fisker, F.-K. Thielemann, and M. Wiescher, Astrophys. J. Lett. **608L**, 61 (2004).
- [8] D. K. Galloway *et al.*, Astrophys. J. **601**, 466 (2004).
- [9] O. Koike, M. Hashimoto, K. Arai, and S. Wanajo, Astron. Astrophys. **342**, 464 (1999).
- [10] B. A. Brown, R. R. C. Clement, H. Schatz, A. Volya, and W. A. Richter, Phys. Rev. C **65**, 045802 (2002).
- [11] S. E. Woosley *et al.*, Astrophys. J. Suppl. **151**, 75 (2004).
- [12] T. Rauscher, F.-K. Thielemann, and K.-L. Kratz, Phys. Rev. C **56**, 1613 (1997).
- [13] B. A. Brown and B. H. Wildenthal, Annu. Rev. Nucl. Part. Sci. **38**, 29 (1988).
- [14] H. Herndl *et al.*, Phys. Rev. C **52**, 1078 (1995).
- [15] M. Honma, T. Otsuka, B. A. Brown, and T. Mizusaki, Phys. Rev. C **65**, 061301(R)(2002).
- [16] M. Honma, T. Otsuka, B. A. Brown, and T. Mizusaki, Phys. Rev. C **69**, 034335 (2004).
- [17] J. L. Fisker *et al.*, At. Data Nucl. Data Tables **79**, 241 (2001).
- [18] H. Schatz *et al.*, Phys. Rev. Lett. **79**, 3845 (1997).
- [19] C. Iliadis *et al.*, Astrophys. J. Suppl. **134**, 151 (2001).
- [20] W. A. Fowler and F. Hoyle, Astrophys. J. Suppl. **9**, 201 (1964).
- [21] G. Audi, A. H. Wapstra, and C. Thibault, Nucl. Phys. **A729**, 337 (2003).
- [22] C. A. Bertulani, Comput. Phys. Commun. **156**, 123 (2003).
- [23] W. A. Fowler, G. R. Caughlan, and B. A. Zimmerman, Annu. Rev. Astron. Astrophys. **5**, 525 (1967).
- [24] G. Vancraeynest *et al.*, Phys. Rev. C **57**, 2711 (1998).
- [25] W. A. Fowler, G. R. Caughlan, and B. A. Zimmerman, Annu. Rev. Astron. Astrophys. **13**, 69 (1975).
- [26] R. A. Ward and W. A. Fowler, Astrophys. J. **238**, 266 (1980).
- [27] B. A. Brown and W. A. Richter, Jour. of Physics: Conference Series **20**, 145 (2005).
- [28] S. Kahn *et al.*, Nucl. Phys. **A481**, 253 (1988).
- [29] B. A. Brown, W. A. Richter, R. E. Julies, and B. H. Wildenthal, Ann. Phys. (NY) **182**, 191 (1988).
- [30] B. H. Wildenthal, in “Elementary Modes of Excitation in Nuclei,” *Proceedings of the International School of Physics “Enrico Fermi,”* course 69, edited by A. Bohr and R. A. Broglia (North-Holland, Amsterdam, 1977), p. 383; B. H. Wildenthal and W. Chung, in *Mesons in Nuclei*, edited by M. Rho and D. H. Wilkinson, (North-Holland, Amsterdam, 1979), p. 723.
- [31] T. Rauscher and F.-K. Thielemann, At. Data Nucl. Data Tables **75**, 1 (2000).
- [32] C. Angulo *et al.*, Nucl. Phys. **A656**, 3 (1999).